

Modeling and Analysis of the Parasitic Series Resistance in Raised Source/Drain FinFETs with Polygonal Epitaxy

Chang-Woo Sohn, Chang Yong Kang, Rock-Hyun Baek, Paul Kirsh and Raj Jammy
SEMATECH, Albany, NY 12203, USA
sohncw@postech.ac.kr

Myung-Dong Ko, Do-Young Choi, Hyun Chul Sagong, Eui-Young Jeong, Chang-Ki Baek, Jeong-Soo Lee and Yoon-Ha Jeong

Dept. of Electrical Engineering, Pohang University of Science and Technology, Pohang, 790-784, South Korea
yhjeong@postech.ac.kr

Jack C. Lee

Dept. of Electrical and Computer Engineering, University of Texas at Austin, Austin, TX 78758, USA

Abstract—In this work, the parasitic series resistance in raised source/drain (S/D) FinFETs with polygonal epitaxy is modeled and analyzed. Specifically, a contact resistance model is developed based on the transmission line theory and geometric transformation to test variously shaped S/D epitaxy formations. Results are verified by comparisons with two- and three-dimensional device simulations. Designs to reduce series resistance are also discussed.

Keywords—Contact resistance, FinFET, polygonal shape, raised source drain, series resistance, transmission line theory

I. INTRODUCTION

To maintain CMOS scaling beyond the 22-nm node, fin-based multiple-gate field-effect transistors (FinFETs) are attractive options. Wrapping the multiple-gate around the fin channel provides excellent electrostatics, which allow using a shorter effective gate length and lower channel doping at the same off-current [1]. Detractors are fabrication complexity and burdens to parasitic components, i.e., parasitic capacitance and series resistance (R_{series}). The parasitic contributions furthermore increase as the gate pitch is scaled [2].

The high R_{series} of FinFETs primarily originates from the need for a narrow fin. One way to reduce R_{series} is to make the fin outside the gate region (i.e., the source/drain (S/D) extension) thicker using silicon epitaxial growth [3], [4]. The silicon epitaxy of the raised S/D is equivalent to a highly doped S/D region in conventional planar FETs; it also widens the silicide-to-silicon interfacial contact area, generating less contact resistance (R_{con}).

Several researchers have analyzed the R_{series} in raised S/D FinFETs using analytic models [5], [6], but in most works a rectangular epitaxy is assumed (Fig. 1 (a) or (b)). The most practical shape is not rectangular but trapezoidal or polygonal (Fig. 1 (c)), since the silicon deposition rate is a function of the

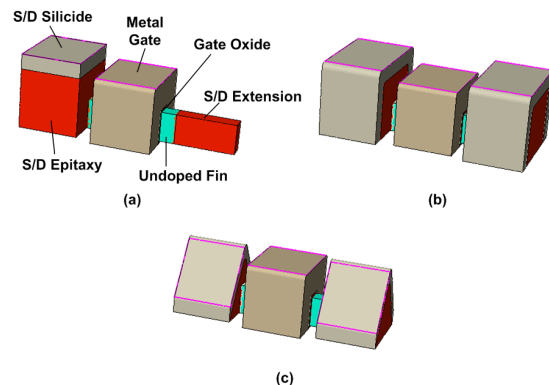


Figure 1. Three dimensional view of three FinFETs including (a) a rectangular shaped epitaxy with top silicide, (b) a rectangular shaped epitaxy with surrounding silicide, (c) a polygonal epitaxy with top silicide. In (a), the epitaxy and silicide from one S/D side are omitted for clarity.

crystal orientation of the fin and the fin doping status [3]. It has also been reported that diamond-shaped epitaxy produces better R_{series} than flat-top epitaxy due to its wider silicide-to-silicon contact area and shorter carrier path [7]. This work, therefore, analyzes R_{series} in raised S/D FinFETs using a simple model for polygonal epitaxy.

II. SERIES RESISTANCE MODEL

A. Modeling Methodology

The R_{series} in raised S/D FinFETs is divided into three major components according to current flows: spread resistance between the channel layer and the fin beneath the sidewall spacer (R_{sp}), sheet resistance of the fin beneath the sidewall spacer (R_{sh}), and contact resistance between the epitaxy and the silicide (R_{con}) as shown in Fig. 2 (a). As the fin is typically

This work was supported by the Ministry of Knowledge Economy, Korea under the IT Consilience Creative program supervised by the National IT Industry Promotion Agency (Project No. C1515-1121-0003), by the World Class University program funded by the Ministry of Education, Science and Technology (Project No. R31-2008-000-10100-0), by the BK21 program and by the National Center for Nanomaterials Technology (NCNT), Korea.

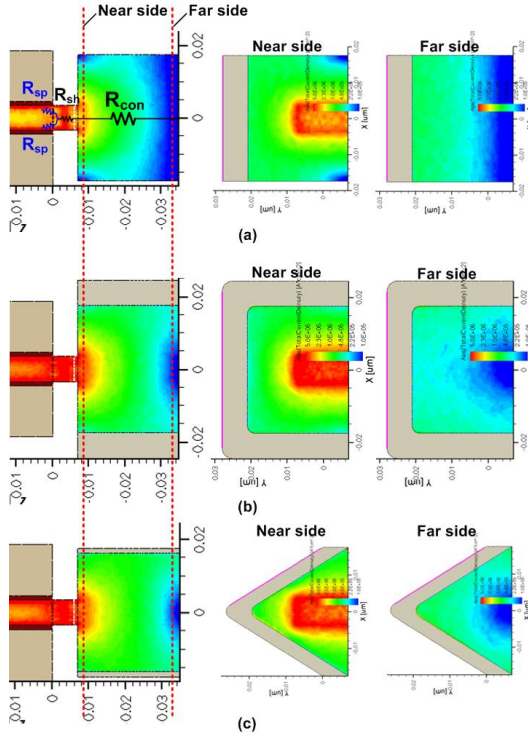


Figure 2. Current density distribution of three FinFETs including (a) a rectangular epitaxy with top silicide, (b) a rectangular epitaxy with surrounding silicide, (c) a polygonal epitaxy with top silicide. Left cross-sections are top-views cut by the half point of the fin height. Middle and right cross-sections are cut by a few nanometers from the end of the sidewall spacer (near side) and the end of the epitaxy region (far side), respectively.

rectangular, the R_{sp} and R_{sh} can be simply evaluated as in [5] and will not be treated here. Because the R_{con} , which depends on the epitaxy shape, is a dominant component in the R_{series} , it will be modeled in detail.

Despite various epitaxy shapes and silicide methods, we have a common observation about current density distribution from the device simulation (Fig. 2). When the epitaxy cross-section is cut close to the end of the sidewall spacer (the near side of the fin), the current density distribution depends on the S/D extension and silicide-to-silicon contact geometry. When the epitaxy cross-section is cut close to the end of the epitaxy region (the far side of the fin), the current density distribution depends on the epitaxy and contact geometry; in this case, the extension geometry does not affect the distribution. Therefore, the R_{con} model is developed considering these two different effects.

B. Contact Resistance – Part I

Our model for the R_{con} basically follows the transmission line theory [8] as shown in Fig. 3 (a). We assume that the current flows uniformly through the S/D extension and partially spreads out from there to the contact area. As the transmission line theory assumes only a one-dimensional

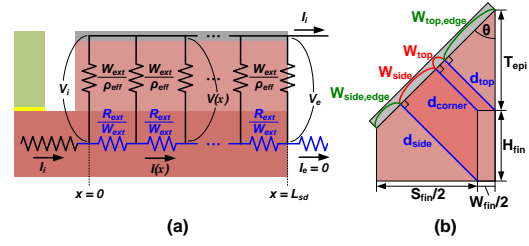


Figure 3. Schematic diagram of the epitaxy cross-section (a) along the channel current direction and (b) perpendicular to the channel current direction. In (a), an equivalent circuit for the transmission line theory is drawn. In (b), geometric notations used for the $R_{con,I}$ expression are indicated.

current flow, we need to make the geometry of the contact surface equivalent to that of the extension surface. To do so, an effective interface resistivity (ρ_{eff}) is introduced instead of using the interface resistivity (ρ_{int}) directly. The ρ_{eff} is expressed in (1)-(5) as follows:

$$\rho_{eff} = \left(\rho_{top}^{-1} + \rho_{side}^{-1} + \rho_{top,edge}^{-1} + \rho_{side,edge}^{-1} \right)^{-1}, \quad (1)$$

$$\rho_{top} = \left(\rho_{int} + d_{corner} \cdot \rho_{epi} \right) \cdot \left(W_{ext} / W_{top} \right), \quad (2)$$

$$\rho_{side} = \left(\rho_{int} + d_{corner} \cdot \rho_{epi} \right) \cdot \left(W_{ext} / W_{side} \right), \quad (3)$$

$$\rho_{top,edge} = \left(\rho_{int} + d_{top} \cdot \rho_{epi} \right) \cdot \left(W_{ext} / W_{top,edge} \right), \quad (4)$$

$$\rho_{side,edge} = \left(\rho_{int} + d_{side} \cdot \rho_{epi} \right) \cdot \left(W_{ext} / W_{side,edge} \right). \quad (5)$$

ρ_{epi} is the resistivity of the epitaxial region. The units of ρ_{eff} , ρ_{int} , and ρ_{epi} are $\{\Omega \cdot \text{cm}^2\}$, $\{\Omega \cdot \text{cm}^2\}$, and $\{\Omega \cdot \text{cm}\}$, respectively. The d_{corner} , d_{top} , and d_{side} are distances from the extension surface to the contact surface, and the W_{top} , W_{side} , $W_{top,edge}$ and $W_{side,edge}$ are width segments of the contact surface as shown in Fig. 3 (b). The geometric notations can be rewritten as functions of epitaxy thickness (T_{epi}), fin height (H_{fin}), fin width (W_{fin}), fin spacing (S_{fin}), and the angle between the contact surface and symmetry axis (θ). Also, W_{ext} is an extension surface width defined as $H_{fin} + 0.5W_{fin}$. When the prefactors in (2)-(5) approximate the ρ_{int} , equation (1) is simplified as

$$\rho_{eff} = \frac{\rho_{int} \cdot W_{ext}}{W_{top} + W_{side} + W_{top,edge} + W_{side,edge}}. \quad (6)$$

Once the ρ_{eff} is obtained, the $R_{con,I}$ can be evaluated using the transmission line theory from (7) and (8) expressed as

$$R_{con,I} = \sqrt{\frac{R_{ext} \cdot \rho_{eff}}{W_{ext}^2}} \coth \left(\frac{L_{sd}}{L_{transfer,I}} \right), \quad (7)$$

$$L_{transfer,I} = \sqrt{\rho_{eff} / R_{ext}}. \quad (8)$$

The R_{ext} is the sheet resistance of the extension, whose unit is $\{\Omega\}$. The L_{sd} is a contact length; $L_{transfer,I}$ is a characteristic length corresponding to the $R_{con,I}$.

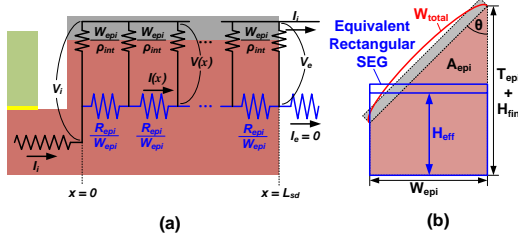


Figure 4. Schematic diagram of the epitaxy cross-section (a) along the channel current direction and (b) perpendicular to the channel current direction. In (a), an equivalent circuit for the transmission line theory is drawn. In (b), geometric notations used for the $R_{con,II}$ expression are indicated.

C. Contact Resistance – Part II

As shown in Fig. 2, the current density distribution gradually changes from being dependent on the S/D extension and contact geometry to the epitaxy and contact geometry. To address the latter effect, the transmission line theory is once again applied as shown in Fig. 4 (a). Contrary to Fig. 3 (a), we assume that the current flows uniformly through the entire epitaxial region and partially spreads out to the silicide contact. Although ρ_{int} is used directly, we still need to make the geometry of the polygonal epitaxy equivalent to that of the rectangular epitaxy with top silicide. To do so, an effective epitaxy height (H_{eff}) is introduced. The H_{eff} is semi-empirically defined as A_{eff}/W_{total} where A_{eff} is a cross-sectional area of polygonal epitaxy and W_{total} is the width of the contact surface (Fig. 4 (b)). Note that as θ decreases, A_{eff} decreases resulting in a shorter H_{eff} .

The equivalent rectangular epitaxy with the H_{eff} and an epitaxy width (W_{epi}) enables us to model the $R_{con,II}$ by the transmission line theory as in

$$R_{con,II} = \sqrt{\frac{R_{epi} \cdot \rho_{int}}{W_{epi}^2}} \coth\left(\frac{L_{sd}}{L_{transfer,II}}\right), \quad (9)$$

$$L_{transfer,II} = \sqrt{\rho_{int} / R_{epi}}. \quad (10)$$

The R_{epi} is the sheet resistance of the epitaxy, whose unit is $\{\Omega\}$. It is defined as ρ_{epi}/H_{eff} . The $L_{transfer,II}$ is a characteristic length corresponding to $R_{con,II}$.

Finally, epitaxy- and contact-geometry-dependent R_{con} is obtained by combining $R_{con,I}$ and $R_{con,II}$ with a weight parameter (α) as follows:

$$R_{con} = \frac{R_{con,I} + \alpha \cdot R_{con,II}}{1 + \alpha} \quad (11)$$

III. EXPERIMENTAL RESULTS AND DISCUSSION

Two- (2-D) and three-dimensional (3-D) TCAD simulations were run to analyze the R_{series} in raised S/D FinFETs. The 2-D simulation is intended to obtain the ρ_{eff} , which transforms the contact surface geometry into the extension surface geometry (Fig. 5). The experimental ρ_{eff} is extracted from the inverse slope of the I-V curves. The 3-D simulation is intended to obtain the R_{series} of FinFETs with

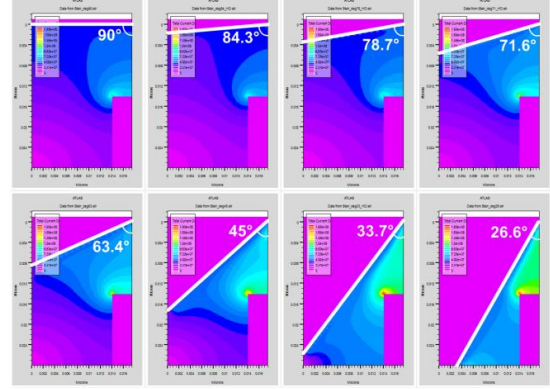


Figure 5. A series of current density distributions in the epitaxy cross-section perpendicular to the channel current direction. The angle between the contact surface and symmetry axis in the polygonal epitaxy is varied.

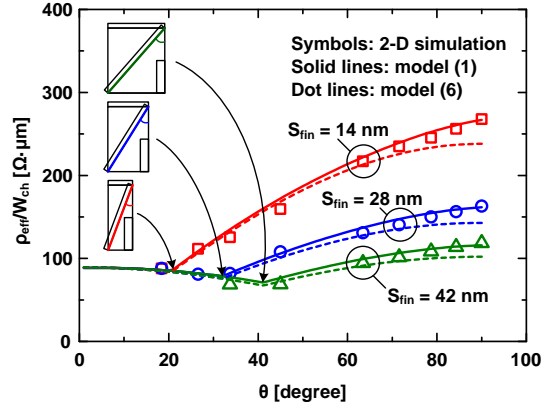


Figure 6. Effective interface resistivity (ρ_{eff}) plotted against the angle between the contact surface and symmetry axis in the polygonal epitaxy. The fin spacing (S_{fin}) is also varied. Insets show the epitaxy cross-sections at which the ρ_{eff} becomes the minimum for each S_{fin} .

variously shaped epitaxy (Fig. 1). The experimental R_{series} is extracted from the $I_{DS}-V_{GS}$ characteristics by obtaining the total resistances and applying a first-order exponential curve fitting [5].

During the simulation, the drift-diffusion model and the continuity and Poisson's equations were used for carrier transport; the doping concentration for the extension and epitaxial regions was set to 10^{20} cm^{-3} . Table I summarizes the geometric and material parameters used in this work.

Fig. 6 shows the simulated and modeled ρ_{eff} as functions of θ and S_{fin} . For convenience, the ρ_{eff} is normalized by an effective channel width (W_{ch}) defined as $2H_{fin}+W_{fin}$. Both (1) and (6) models generally agree well with the simulation results, but model (1) yields the results closer to the simulation. ρ_{eff} is found to decrease when decreasing θ from 90 degrees, which is attributed to the increment in the contact surface width providing more conduction paths as shown in Fig. 5. The contact surface width is maximized when

TABLE I. PARAMETERS USED IN THIS WORK

Geometric Parameters				
H_{fin}	W_{fin}	S_{fin}	T_{epi}	L_{sd}
14 nm	7 nm	14 nm	14 nm	28 nm
Material Parameters				
ρ_{int}	ρ_{epi}	R_{ext}		
$2 \cdot 10^{-8} \Omega \cdot \text{cm}^2$	1025 $\mu\Omega \cdot \text{cm}$	3.66 k Ω		

$$\theta = \tan\left(\frac{0.5(W_{fin} + S_{fin})}{T_{epi} + H_{fin}}\right), \quad (12)$$

and thus the ρ_{eff} is minimized at this point (inset of Fig. 6). As θ decreases beyond this point, ρ_{eff} increases slightly due to the narrower contact surface. Note that the carrier path distance from the extension to the contact area has little impact on ρ_{eff} . Even though it is included in (2)-(5), ρ_{epi} multiplied by the distance is much smaller than the ρ_{int} .

Fig. 7 shows the simulated and modeled R_{series} components as a function of θ . The R_{series} is also normalized by W_{ch} for convenience. The modeled R_{series} as a sum of R_{sp} , R_{sh} , and R_{con} from (11) shows excellent agreement with the simulation results. Note that the modeled $R_{con,I}$ as in (7) shows a similar dependence of ρ_{eff} on θ ; as θ decreases from 90 degrees, the $R_{con,I}$ decreases to the minimum point and then increases slightly. In the simulation, however, the R_{series} increases sharply after the minimum point, which cannot be predicted using the model (7) alone. This feature can be supplemented by the $R_{con,II}$. The epitaxy cross-sectional area decreases drastically after the minimum point of $R_{con,I}$, sharply increasing the $R_{con,II}$.

Our analysis provides S/D design guides to reduce R_{series} . The effective area of the contact surface should be maximized without critically reducing the epitaxy volume. Here, the epitaxy with surrounding silicide (Fig. 1 (b)) is favorable for obtaining the lowest R_{series} as shown in Fig. 8. However, it has limitations in a high density multiple-fin structure. In case that the epitaxy of one fin combines with the epitaxy of adjacent fins, the surrounding silicide is difficult to implement. Polygonal epitaxy with an optimized angle (Fig. 1 (c)), on the other hand, provides lower R_{series} than rectangular epitaxy with top silicide (Fig. 1 (b)); it can also be used in high density multiple-fin structures.

IV. CONCLUSION

We have modeled and analyzed series resistance in FinFETs with a polygonal epitaxy. Despite variously shaped epitaxy and silicide, it is shown that the current density distribution gradually changes from depending on the S/D extension and contact geometry to depending on the epitaxy and contact geometry. Considering this effect, a contact resistance model was developed based on the transmission line theory and geometric transformations. Our model agrees well with 2-D and 3-D TCAD simulation results. Analysis using the model suggests that well-optimized polygonal epitaxy provides low contact resistance even when only the top epitaxial surface is silicided.

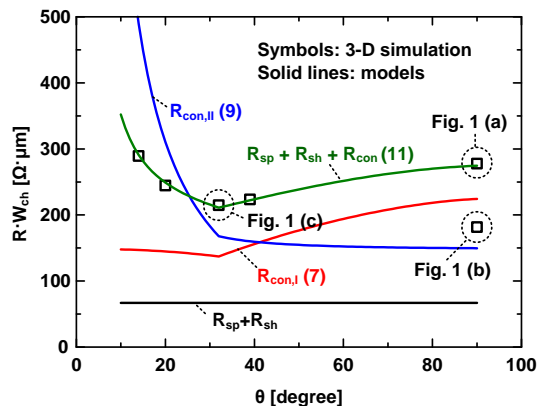


Figure 7. Series resistance components plotted against the angle between the contact surface and symmetry axis in the polygonal epitaxy. Series resistances from the device simulation as shown in Fig. 1 are indicated by the symbols. Modeled contact resistance considering either the contact surface effect or the epitaxy volume effect is indicated by lines.

REFERENCES

- [1] M. Bohr, "The evolution of scaling from the homogeneous era to the heterogeneous era," in *IEDM Tech. Dig.*, 2011, pp. 1–6.
- [2] K. Kuhn, "Moore's crystal ball: Device physics and technology past the 15 nm generation," *Microelectron. Eng.*, vol. 88, pp. 1044–1049, 2011.
- [3] J. Kedzierski, M. Jeong, E. Nowak, T. S. Kanarsky, Y. Zhang, R. Roy, D. Boyd, D. Fried and H.-S. P. Wong, "Extension and source/drain design for high-performance FinFET devices," *IEEE Trans. Electron Devices*, vol. 50, no. 4, pp. 952–958, Apr. 2003.
- [4] A. Dixit, K. G. Anil, R. Rooyackers, F. Leys, M. Kaiser, N. Collaert, K. De Meyer, M. Jurczak and S. Biesemans, "Minimization of specific contact resistance in multiple gate NFETs by selective epitaxial growth of Si in the HDD regions," *Solid State Electron.*, vol. 50, pp. 587–593, 2006.
- [5] A. Dixit, A. Kottantharayil, N. Collaert, M. Goodwin, M. Jurczak, and K. D. Meyer, "Analysis of the parasitic S/D resistance in multiple-gate FETs," *IEEE Trans. Electron Devices*, vol. 52, no. 6, pp. 1132–1140, Jun. 2005.
- [6] D. Tekleab, S. Samavedam and P. Zeitoff, "Modeling and analysis of parasitic resistance in double-gate FinFETs," *IEEE Trans. Electron Devices*, vol. 56, no. 10, pp. 2291–2297, Jun. 2005.
- [7] H. Kawasaki, V. S. Basker, T. Yamashita, C.-H. Lin, Y. Zhu, J. Faltermeier, S. Schmitz, J. Cummings, S. Kanakasabapathy, H. Adhikari, H. Jagannathan, A. Kumar, K. Maitra, J. Wang, C.-C. Yeh, C. Wang, M. Khater, M. Guillorn, N. Fuller, J. Chang, L. Chang, R. Muralidhar, A. Yagishita, R. Miller, Q. Ouyang, Y. Zhang, V. K. Paruchuri, H. Bu, B. Doris, M. Takayanagi, W. Haensch, D. McHerron, J. O'Neill and K. Ishimaru, "Challenges and solutions of FINFET integration in an SRAM cell and a logic circuit for 22 nm node and beyond," in *IEDM Tech. Dig.*, 2009, pp. 1–4.
- [8] H. H. Berger, "Contact resistance on diffused resistors," in *Proc. ISSCC*, 1969, pp. 162–163.